

# Paleocurrent directions from paleomagnetic reorientation of magnetic fabrics in deep-sea sediments at the Antarctic Peninsula Pacific margin (ODP Sites 1095, 1101)

J.M. Parés<sup>\*</sup>, N.J.C. Hassold<sup>1</sup>, D.K. Rea, B.A. van der Pluijm

*Department of Geological Sciences, University of Michigan, Ann Arbor, MI 48109-1005, United States*

Received 24 August 2006; received in revised form 2 April 2007; accepted 4 April 2007

## Abstract

We have determined the azimuth of bottom-current flow in drift deposit sediments recovered at ODP Sites 1095 and 1101, Antarctic Peninsula, using paleomagnetic reorientation of anisotropy of magnetic susceptibility (AMS) ellipsoids. A total of 38 cores from the two ODP sites have been measured, providing spatial and directional information on the physical record of the ACC (Antarctic Circumpolar Current) in the Plio-Pleistocene. Declination and inclination of the paleomagnetic vector of each core segment were used to reorient the AMS principal axes to the geographic coordinates. The cores were reoriented using the measured direction of the characteristic remanent magnetization (ChRM) with respect to a common reference line for the core, from which we are able to determine the orientation of the paleocurrent flow for Sites 1095 (Drift 7) and 1101 (Drift 4) relative to the geographic coordinates. Both sites have paleocurrent directions trending ~NW–SE, which in the former locality are parallel to a sediment wave field. Our study shows that a combination of magnetic fabric analysis and paleomagnetism allows deep-sea sedimentary fabric to be used as a long-term proxy of bottom-current flow history.

© 2007 Elsevier B.V. All rights reserved.

*Keywords:* Antarctica Pacific margin; magnetic anisotropy; ODP; paleocurrent

## 1. Introduction

The physical properties of bottom-current flow recorded by deep-sea sediments can provide information about the evolution of oceanic currents, their strength and direction; information on this latter point forms the basis of this contribution. Specifically, details regarding the ACC (Antarctic Circumpolar Current) significantly affect our understanding of late Cenozoic paleoceanography, as

it is thought to isolate Antarctica from the warmer waters to the north. The anisotropy of magnetic susceptibility (AMS) provides a gauge for sediment fabric that senses the degree of preferred grain orientation in sediments and, hence paleocurrent strength and direction. However these results cannot be placed in a geographic context from core analysis without the use of paleomagnetic data.

Previous workers have applied AMS to sediment samples to determine relative current strength (Ellwood and Ledbetter, 1977, 1979; Ellwood et al., 1979; Joseph et al., 1998, 2004; Hassold et al., 2006), but few have applied this method to determine paleodirections of current flow in sediments (e.g., Ledbetter and Ellwood, 1980; Liu et al., 2001). The high sedimentation rates and

<sup>\*</sup> Corresponding author.

*E-mail address:* jmpares@umich.edu (J.M. Parés).

<sup>1</sup> Current address: Department of Earth and Resource Sciences, University of Michigan-Flint, 303 E. Kearsley Street, Flint, MI-48502.

high concentration of terrigenous material at the drifts along the Antarctic Peninsula (Acton et al., 2002; Hassold, 2006 Chapters 3 and 4) present an opportunity to explore this potentially powerful aspect of fabric study.

Camerlenghi et al. (1997a) identified a number of drifts, or elongate sediment bodies formed by the interaction of terrigenous sediment from the Antarctic Peninsula continental shelf and ocean currents. They used current meters to study the bottom currents along Drift 7, located along the continental rise of the Pacific margin of the Antarctic Peninsula (Fig. 1). The current measurements by Camerlenghi et al. (1997a,b) showed an average current speed of 6 cm/s and a maximum of 20 cm/s — which meets the expectations for building a drift deposit. The currents paralleled the isobaths faithfully, which is what our results show as will be discussed later. The main current flows southwest along the Pacific margin of the Antarctic Peninsula, moving along contours, thus around the several drift lobes. It is a subpolar gyre, with waters derived from the Weddell sea to the east, coming around past the South Scotia Islands.

In this study, we determine the paleoazimuth of bottom-current flow at ODP Sites 1095 and 1101, Antarctic Peninsula (Fig. 1). A total of 39 cores (23 from ODP Site 1095 (206 m core length) and 16 from ODP Site 1101 (136 m core length)) have been analyzed for AMS (Tables 1 and 2, in the electronic supplement), providing directional information on the physical record of the ACC in the Plio-Pleistocene.

## 2. Geological setting

Ocean Drilling Program (ODP) Leg 178 Site 1095 (66°59'S, 78°29'W, 3840 m water depth) was drilled on a sediment drift (Drift 7 (Barker et al., 1999)) along the Pacific margin of the Antarctic Peninsula (Fig. 1). This site is located on the northwest lower margin of the Antarctic Peninsula and is bathed by southwest flowing bottom currents (Camerlenghi et al., 1997a; Pudsey, 2001). Four holes were drilled at Site 1095 to a total depth of 570 m below sea floor (mbsf). In general, the sediments were diatom-bearing silty clay and clay, with some siliceous ooze and sand. The oldest of these sediments was late Miocene.

Site 1101 (latitude 64°22.3'S, longitude 70°15.6'W, 3280 m (Barker and Camerlenghi, 2002)) is located on Drift 4 along the Pacific margin of the Antarctic Peninsula, on the northwest flank of the continental rise, north of Drift 7. Only one hole was drilled at Site 1101, to 217.7 mbsf, and recovered clayey silt, silt, foraminiferous clay and diatom ooze ranging in age from late Pliocene through Holocene. Both sites are

under the depositional influence of the Antarctic Peninsula Ice Cap and record effects of climate changes on the Ice Cap, as well as the effects of sea ice (Bart and Anderson, 2002; Barker and Camerlenghi, 2002).

### 2.1. Anisotropy of magnetic susceptibility (AMS) and paleocurrents-principles

The low field magnetic susceptibility (MS) of a rock results from the total contribution of its bulk mineralogy, including paramagnetic (e.g., phyllosilicates, iron-bearing silicates in general), diamagnetic (e.g., quartz, calcite) and ferromagnetic (*sensu lato*) (e.g., magnetite, goethite, hematite) grains. An intrinsic property of most rock-forming minerals is that magnetic susceptibility is anisotropic (Nye, 1957) and defined as  $K_{ij} = M_i / H_j$ . For example, mica grains show a close relationship between the crystallographic (001) direction and mineral shape as well as between crystallographic *c*-axis and the minimum susceptibility direction (Richter et al., 1993). Magnetic fabric, therefore, is directly related to preferred orientation of mica grains if the susceptibility is dominated by this mineral phase. The AMS in rocks depends mostly on crystallographic preferred orientation, compositional layering, distribution and size of microfractures and the shape fabric of grains.

AMS defines a symmetric, second-rank tensor that has six independent matrix elements. When the coordinate system is referred to the eigenvectors, they describe an ellipsoid that is termed the magnitude ellipsoid (Nye, 1957), whose semi-axes are the three principal susceptibilities (maximum, intermediate and minimum susceptibility axes, or  $K_{\max}$ ,  $K_{\text{int}}$  and  $K_{\min}$  hereafter) (Table 1, in the electronic supplement). AMS has been used as a tool in the analysis of petrofabrics since Ising (1942) first proposed its application to geology, and it has successfully been used since then to investigate the spatial and geometrical configuration of the rock components for qualitative estimation of fabric development (reviews by (Hrouda, 1982; McDonald and Ellwood, 1987; Borradaile, 1988; Tarling and Hrouda, 1993)). Determination of preferred orientation in minerals is necessary information in a variety of studies ranging from structural geology (e.g., (Housen and van der Pluijm, 1990; Parés et al., 1999; Scott and Benn, 2001; Neves et al., 2003; Parés and van der Pluijm, 2003)) to sedimentary depositional environments (e.g., (Graham, 1954; Kent and Lowrie, 1975; Ellwood et al., 1979; Hounslow, 1985; Kodama and Sun, 1990; Joseph et al., 1998; Park et al., 2000)).

In both terrigenous sedimentary rocks and laboratory experiments (e.g., (Rees and Woodall, 1975); summary

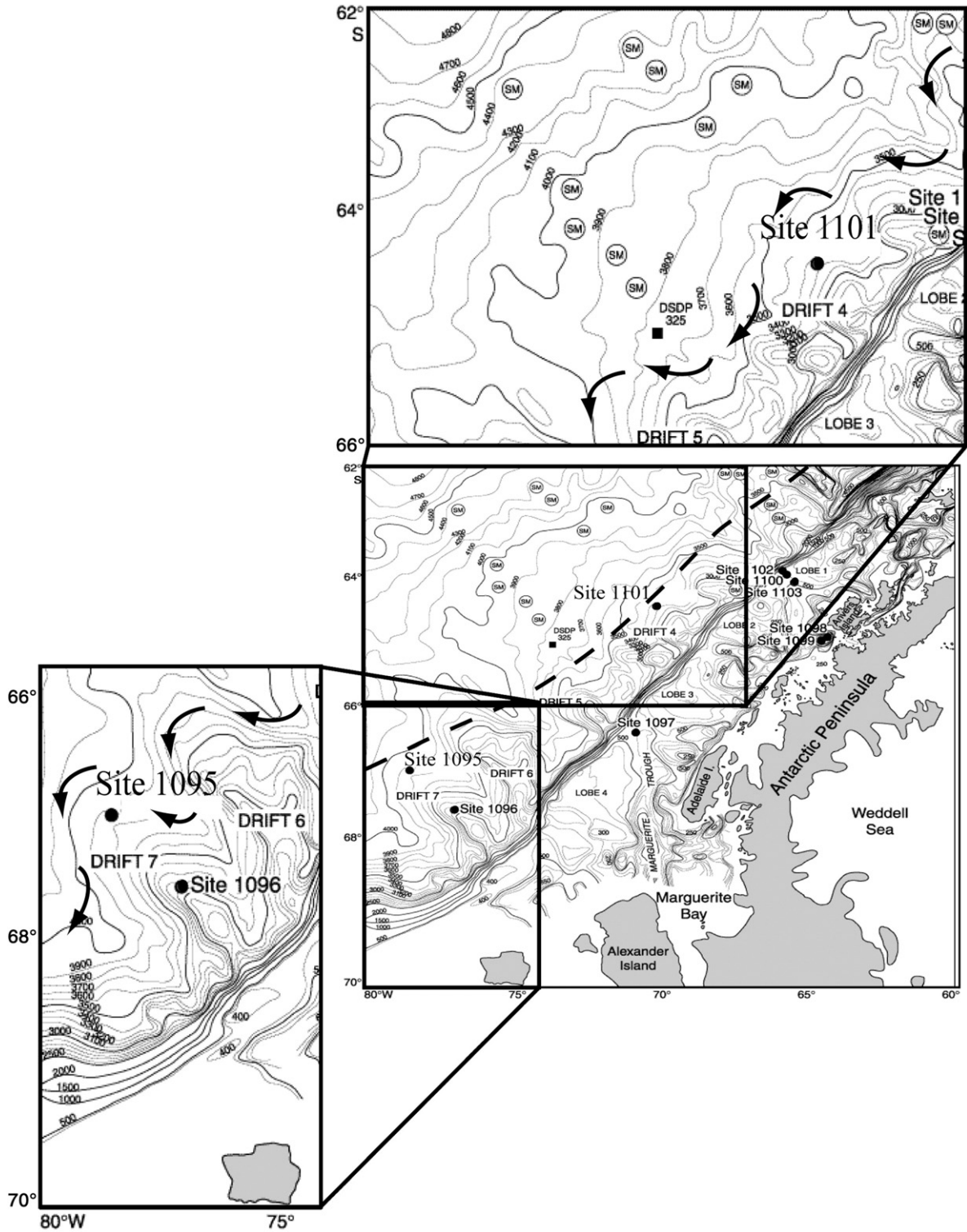


Fig. 1. Leg 178 drillsites along the Antarctic Peninsula. Sites 1101 and 1095 are located on Drifts 4 and 7 respectively. The location of the contour current is shown by the large arrows in the insets. Notice contour currents generally flowing southwest. Based on data from Uenzelmann-Neben (2006).

in Tarling and Hrouda, 1993), it has been observed that the AMS axes distribution reflects the depositional plane in sediments (see review in Tarling and Hrouda, 1993). Thus, the magnetic foliation (i.e., plane containing  $K_{\max}$  and  $K_{\text{int}}$  axes) is typically parallel to the depositional surface and the magnetic lineation (cluster of  $K_{\max}$  axes) is parallel or normal to the paleocurrent direction, depending on the hydrodynamic regime (moderate or high velocity respectively). There is a wide variety of parameters that have been used to describe the axial magnitude relationships of the susceptibility ellipsoid (see also Tauxe, 1998). These include the axial ratios  $L$  ( $K_{\max}/K_{\text{int}}$ ),  $F$  ( $K_{\text{int}}/K_{\text{min}}$ ),  $P$  or degree of anisotropy  $P' = \exp(2(a_1^2 + a_2^2 + a_3^2))^{1/2}$  where  $a_1 = \ln(K_{\max}/K_b)$ , etc. and  $K_b = (K_{\max} + K_{\text{int}} + K_{\text{min}})/3$  and eccentricity  $T = 2(\ln K_{\text{int}} - \ln K_{\text{min}}) / (\ln K_{\max} - \ln K_{\text{min}}) - 1$  to define the degree to which the ellipsoid is oblate or prolate (Jelinek, 1981).

### 3. Methodology

One hundred forty-six samples from 20 cores from Site 1095 were taken from the working half of cores 1095A1H to 1095A10H and 1095B1H to 1095B13H at the ODP Bremen Repository. This resulted in a sampling frequency of 40 ky based on the magnetic stratigraphy (Acton et al., 2002). One hundred sixty-six samples were taken from cores from Site 1101. Of these samples, 163 were taken from the u-channels from the top 15 cores and 3 were taken from core 16H by the staff of the ODP Bremen Repository. The average sampling frequency over the 16 cores was 12 ky. Because of coring disturbances, the top 20 m of the core from Site 1101 was less densely sampled. Standard  $2 \times 2 \times 2$  cm plastic cubes were used and

taken either from the working half cores or u-channels. Particular attention was paid in completely filling the cubes with sediment, as sample shape is critical in AMS studies.

All AMS measurements were carried out with a Kappabridge KLY-2.03 susceptibility bridge (Geofyzika Brno) at the University of Michigan, using the fifteen directional susceptibilities scheme of Jelinek (1978), at a frequency of 920 Hz (sensitivity of the coil is  $\sim 5 \times 10^{-7}$  SI). AMS data analysis was performed by linear perturbation analysis (LPA, Tauxe, 1998), following the method initially developed by Constable and Tauxe (1990) for statistical bootstrapping of anisotropy data in order to obtain the confidence ellipses. First, the matrix elements and residual errors for each individual sample are calculated using fifteen measurements. Then, the bootstrap statistics for the matrix elements are calculated. The data for used individual localities are listed in Table 1 (in the electronic supplement), including the values and orientation for the principal, major and minor eigenvectors and associated eigenvalues.

Some authors have pointed out that sometimes preferred orientations of the principal axes of susceptibility are artifacts of coring and sampling (e.g., Copons et al., 1997; Aubourg and Oufi, 1999). We have plotted the orientation of the principal AMS axes in sample coordinates to test such a possibility (Fig. 2) and the axes distribution shows no pattern consistent with a coring or sampling induced magnetic fabrics. Typical laboratory-induced fabrics produce  $\sim$ E–W trending  $K_{\max}$  axes (e.g., Copons et al., 1997) and/or  $\sim$ N–S trending  $K_{\text{min}}$  axes (e.g., Aubourg and Oufi, 1999) in geographic coordinates, as opposed to the axes distribution observed in our data set. The method of paleomagnetic core reorientation aligns the direction of

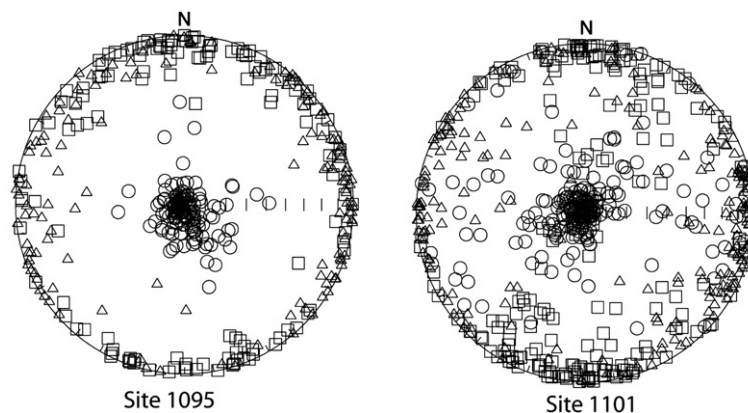


Fig. 2. Orientation of the principal axes of susceptibility in sample coordinates. Squares, triangles and circles represent maximum, intermediate, and minimum axes of susceptibility respectively.

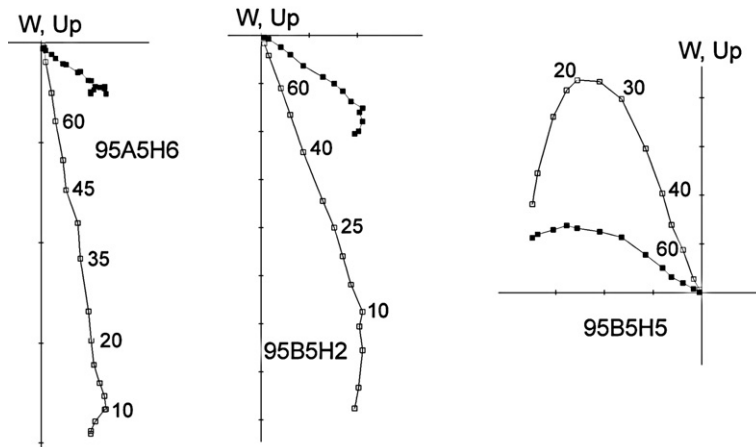


Fig. 3. Representative orthogonal demagnetization diagrams for Site 1095 samples. Full (open) symbols represent projection on to the horizontal (vertical) plane. Alternating field demagnetization steps are shown in mTesla.

remanent magnetization (RM) within the cored formation to define the direction of the geomagnetic field at the time of magnetization of the sediment. The direction of stable RM is determined with respect to a common reference line that is scribed along the length of the core. The orientation of the paleomagnetic vector is then used to reorient the core and any associated directional properties (such as AMS). The rotation of the core relative to the geographic coordinates is specified by the angle between the horizontal component of the mean characteristic RM direction (ChRM) and the reference line.

Paleomagnetic analysis was carried out using a three-axis 2G SQUID magnetometer housed in a field-free room at the University of Michigan. Noise level of the magnetometer is  $\sim 7 \times 10^{-6}$  A/m, well below the magne-

tization intensity of the measured samples. Specimens were stepwise demagnetized in a Sapphire Alternating Field Demagnetizer, capable of producing fields up to 200 mT. ChRM component directions were calculated for all specimens using principal component analysis (Kirschvink, 1980), guided by visual inspection of orthogonal demagnetization plots (Zijderveld, 1967) (Fig. 3). We have used the statistical bootstrap technique adapted for paleomagnetic vectors by Tauxe (1998) in order to estimate mean directions and associated Fisher parameters, which has the advantage of not assuming any prior distribution for the data considered. For Sites 1095A and 1095B, we have combined measurements made at the Paleomagnetism Laboratory, University of Michigan, and data obtained at the Core Repository Janus database (<http://www-odp.tamu.edu/database>). Details of the

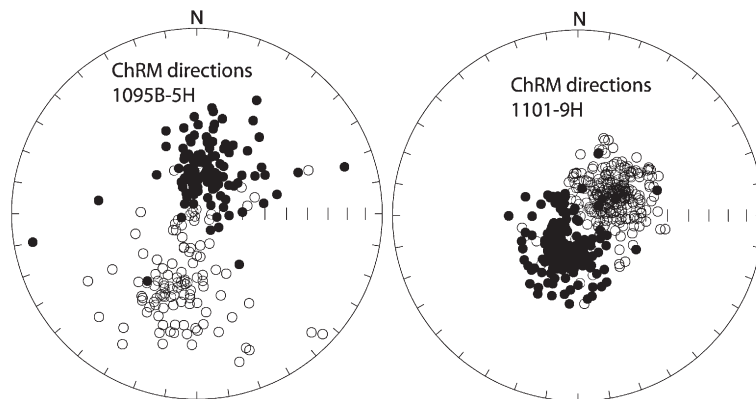


Fig. 4. Stereographic projections of Characteristic Remanent Magnetization (ChRM) directions for two representative cores. Dots (circles) represent directions in the lower (upper) hemisphere. Notice the presence of both normal (circles) and reverse (dots) magnetization directions.

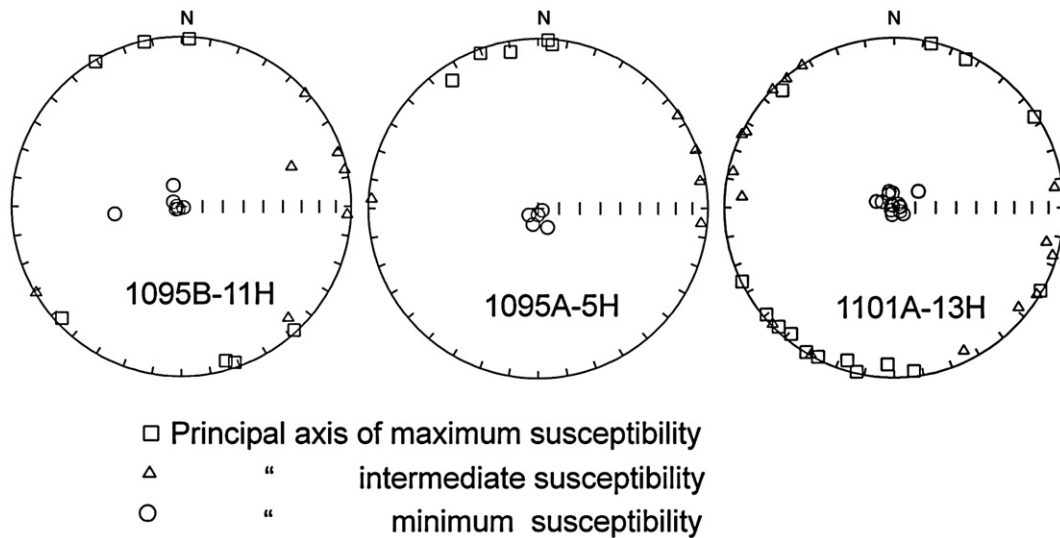


Fig. 5. Representative stereographic projections of principal axes of magnetic anisotropy, in sample coordinates. Each plot corresponds to a given core. Notice vertical minimum axes of susceptibility, consistent with a depositional, sedimentary fabric. See text for discussion.

paleomagnetic and rock magnetic properties of Site 1095 are given in [Barker and Camerlenghi \(2002\)](#) and [Acton et al. \(2002\)](#). For Site 1101, we have used the paleomagnetic data from [Guyodo et al. \(2001\)](#) where details on the demagnetization and rock-magnetism can be found. The paleomagnetic data for Site 1101 u-channel samples are

available in ASCII tables in [Acton et al. \(2002\)](#). For each core, mean paleomagnetic directions were computed for both polarities ([Fig. 4](#), Table 3, in the electronic supplement). The mean declination was then aligned with the geographic north and the resulting angle was used as a rotation parameter for the AMS fabric.

Table 1  
 Summary of the anisotropy of magnetic susceptibility of sites used in this study

Core			Eigenvector 1					Eigenvector 3				
	<i>N</i>	$\tau$	$\sigma$	Dec	Inc	Dec'	$\tau$	$\sigma$	Dec	Inc	Dec'	$\rho$
1095A-02H	5	0.33827	0.00137	4.6	1.6	312	0.32529	0.00276	164.2	88.3	112	-52
1095A-05H	6	0.34008	0.00098	345.8	4.9	171	0.32090	0.00197	182.7	84.9	8	-175
1095A-06H	6	0.34240	0.00173	42.2	4.3	150	0.31691	0.00272	152.6	77.8	261	+108
1095A-08H	5	0.34155	0.00110	10.7	3.3	301	0.31885	0.00227	256.0	82.1	78	+290
1095A-09H	6	0.34359	0.00058	35.1	14.2	159	0.31503	0.00092	174.4	71.6	298	+124
1095B-05H	7	0.34217	0.00173	4.8	7.8	172	0.31889	0.00302	134.7	78	251	+167
1095B-06H	9	0.34074	0.00124	350.1	8.2	182	0.32185	0.00209	121.1	77.6	313	-168
1095B-08H	7	0.34306	0.00241	144.7	3.1	290	0.31525	0.00471	282.2	85.7	67	+145
1095B-10H	6	0.34088	0.00158	177.6	4.4	326	0.32031	0.00259	333.7	85.1	122	+148
1095B-11H	7	0.34085	0.00235	159.6	0.8	297	0.31945	0.00448	272.3	88	49	+137
1095B-13H	4	0.34870	0.00069	62.9	2	335	0.30305	0.00191	205.9	87.5	118	+272
1101A-03H	16	0.34316	0.00173	208.3	27.7	301	0.32578	0.00138	47.4	61.0	140	+93
1101A-07H	9	0.33552	0.00107	187.2	2.1	309	0.33099	0.00177	292.4	82.1	54	+122
1101A-08H	8	0.33766	0.00095	2.0	1.5	241	0.32771	0.00171	156.4	88.3	36	+239
1101A-09H	12	0.33872	0.00130	176.1	5.4	314	0.32492	0.00221	330.8	84.0	109	+138
1101A-10H	14	0.33916	0.00111	8.0	3.8	262	0.32333	0.00215	225.8	85.2	120	+254
1101A-12H	16	0.33741	0.00093	187.7	3.4	335	0.32649	0.00180	323.3	85.2	110	+147
1101A-13H	15	0.34028	0.00059	203.1	2.5	287	0.32060	0.00112	10.7	87.5	95	+84
1101A-14H	14	0.34099	0.00091	174.0	3.8	358	0.31866	0.00171	328.2	85.8	152	+184

Symbols:  $\tau$  — eigenvalues;  $\sigma$  — standard deviation;  $\rho$  — angle of rotation (as deduced from paleomagnetic data, see Table 3 in the electronic supplement), Dec/Inc — Declination and Inclination of the mean axes, Dec' — Declination after rotation by the angle  $\rho$ , *N* — Number of samples used. Eigenvectors 1 and 2 refer to the maximum and minimum principal axes of susceptibility respectively.

Because AMS analysis is a non-destructive technique, as opposed to paleomagnetism, we first measured bulk susceptibility and AMS of the samples after which the NRM and progressive AF demagnetization was applied.

### 3.1. Fabric and flow along the Antarctic Peninsula

Because ODP holes are typically drilled and recovered in successive 9.5 meter-long cores, which are not oriented relative to each other, we have based our analysis on samples grouped by cores (Tables 1 and 3, in the electronic supplement). Analysis and interpretation of the sedimentary fabric is based on the orientation distribution of the principal AMS axes. For the most part, sediments show  $K_{\max}$  axes that are distributed within the depositional plane and  $K_{\min}$  axes perpendicular to it, resulting in oblate magnetic ellipsoids (Fig. 5). This configuration is interpreted as particles that are aligned in a plane that is parallel to the depositional surface where flow is very low or absent. Occasionally,  $K_{\max}$  axes tend to cluster, producing higher values of magnetic lineation, while  $K_{\min}$  axes are slightly off-vertical. Such an ellipsoid distribution has been interpreted as produced by moderate velocity currents that occasionally produce an upstream imbrication of the grains (e.g., Rees and Woodall, 1975; Ellwood et al., 1979; Ledbetter and Ellwood, 1980; Liu et al., 2001). We have calculated the mean direction of the  $K_{\max}$  axes where this distribution is observed (Table 1). The orientation of the principal axes in Table 1 (in the electronic supplement) is shown in core coordinates, i.e., the angles are relative to the core coordinate system. In order to determine the azimuth of  $K_{\max}$  axes and hence paleoflow orientation in geographic coordinates, we use the paleomagnetic record of the cores, as explained

above. The assumption is that the mean ChRM represents Earth's axial dipole field, with secular variation averaged out. One caveat in our approach is the high latitude of the drilled sites (64°S and 67°S for 1101 and 1095), which translates into steep magnetic inclinations (76° and 78° respectively). This high value in inclination introduces a larger uncertainty in the restored directions than would be the case at lower latitudes.

After rotating the cores until the horizontal component of the ChRM is aligned with the geographic north, the azimuth of  $K_{\max}$  axes represents the geographically realigned preferred grain orientation and thus the paleoflow trends (Table 1). After reorientation,  $K_{\max}$  axes of different cores show an excellent grouping (Fig. 6), demonstrating that the method is successful in restoring the cores into geographic coordinates. At both Sites 1101 and 1095, the general trend of the  $K_{\max}$  principal AMS axes, and hence the paleoflow direction, is approximately NW–SE. Such AMS fabrics are considered as directional only (as opposed to vectorial), as they give the trend or line of azimuth of the current, but not the upstream direction nor the strength of the current. Site 1095 produces  $K_{\max}$  principal axes plunging in both directions, NW and SE, whereas Site 1101 reveals only NW-plunging  $K_{\max}$  axes. Because processes other than depositional may have occurred (e.g., slightly off-vertical boreholes, sampling error) may have occurred, we cannot reliably use the  $K_{\max}$  plunge to determine the upstream direction.

The general NW–SE azimuth for the flow direction in both localities, as indicated by the AMS axes distribution, is perpendicular to the general trend of the continental shelf. A recent study by Rebesco et al. (2007) allows us to compare the paleocurrent directions at Site

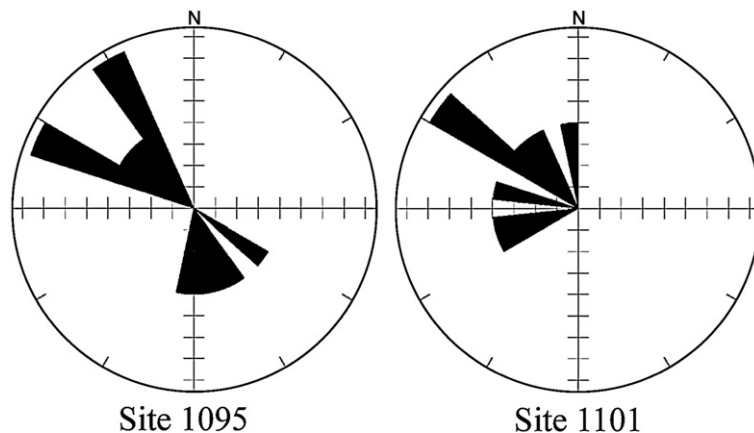


Fig. 6. Rose diagram of maximum susceptibility axes directions for Sites 1095 and 1101. Data shown after paleomagnetic reorientation of the cores. Both sites reveal an approximate paleodirection of ~NW-SE.

1095 with the morphology of the ocean floor. According to these authors, sediment at Drift 7 is interpreted as the product of weak flowing bottom currents pirating the suspended fine material from turbidity currents. The NE side of Drift 7 is characterized by an undulating depositional bedform as revealed by seismic profiles, interpreted as a sediment wave field (Camerlenghi et al., 1997a,b; Rebesco et al., 2007). Just north of Site 1095, the Alexander Channel extends for some 100 km with a NW–SE orientation. Other lineations with a similar orientation are found beyond the distal part of this channel, collectively revealing the presence of morphological features consistent with a NW–SE paleocurrent direction. Our paleomagnetically corrected paleocurrent direction at Site 1095, supports Rebesco's interpretation of a contourite origin for Drift 7, with  $K_{\max}$  axes that are aligned parallel to depth contours.

We do not have sufficiently detailed morphology of the area around Site 1101, Drift 4, to contrast the paleocurrent direction with bedform orientation. However, given that this a drift developed some 200 km NE of Drift 7 on the same continental margin, with similar depositional features, the NW–SE trending paleocurrent direction is similarly interpreted as indicating a contouritic origin for Drift 4.

Magnetic fabric and grain size studies of sediments from Site 1095 indicate a gradual decrease in the current strength over the last 10 my (Hassold, 2006). Similar studies from Site 1101 indicate a relatively constant current at this site for the past 3 my. (Hassold, 2006). All together, this information indicates a current that has, for millions of years, remained essentially unchanged in direction, slightly decreasing in strength at Site 1095 while remaining constant at Site 1101. Hernández-Molina et al. (2006), studying the seismic morphology of a fossil mound sediment body located northeast of Site 1095, have determined that, during the middle to late Miocene, the current changed from a NE flow to the SW of today. Our data support the general sense of this flow, but do not distinguish between the two directions.

#### 4. Summary

Combining paleomagnetism and magnetic fabric analysis provides a powerful tool for determining paleocurrent directions along the Antarctic Peninsula continental margin. Magnetic fabrics of drift sediments generally show a well-preserved depositional fabric, with  $K_{\max}$  axes within the bedding plane and  $K_{\min}$  axes vertical. Using paleomagnetic directions measured for these sediments, we have azimuthally oriented  $K_{\max}$  axes, which are thought to align parallel to the paleocurrent

flow azimuth. At Sites 1095 and 1101, this approach produces a generally NW–SE trending paleoflow direction for the Miocene through the Pleistocene. At Site 1095, Drift 7, this azimuth direction matches the elongation of the sediment wave described by Rebesco et al. (2007), who similarly interpret the sediments as deposited by contour currents rather than by turbidity currents. We similarly interpret the results at Site 1101, which also show a NW–SE trend, as indicative of deposition from contourites.

The agreement between our magnetically determined paleocurrent trends and the detailed morphology of sediment drifts in the Antarctic Peninsula reveals the potential of using magnetic fabric in sediments as proxy for long-term bottom current history. When used in conjunction with grain size and fabric analyses (e.g., Joseph et al., 1998), we can determine a robust record for paleocurrents in space and time.

#### Acknowledgments

We thank the staff of the ODP Bremen Repository for their assistance in procuring the samples, Y. Guyodo for providing the paleomagnetic data for the cores from Site 1101 and M. Rebesco et al. for providing a copy of their 2007 manuscript. We also thank Gary Acton and an anonymous reviewer for providing helpful comments. This work has funded by the NSF Grant OPP-0337091.

#### Appendix A. Supplementary data

Supplementary data associated with this article can be found, in the online version, at [doi:10.1016/j.margeo.2007.04.002](https://doi.org/10.1016/j.margeo.2007.04.002).

#### References

- Acton, G.D., Guyodo, Y., Brachfeld, S.A., 2002. Magnetostratigraphy of sediment drifts on the continental rise of west Antarctica (ODP Leg 178, Sites 1095, 1096, and 1101). *Proc. ODP Sci. Results* 178, 1–61.
- Aubourg, C., Oufi, O., 1999. Coring-induced magnetic fabric in piston cores from the Western Mediterranean. *Proc. ODP Sci. Results* 161, 129–136.
- Barker, P.F., Camerlenghi, A., 2002. Glacial history of the Antarctic Peninsula from Pacific margin sediments. *Proc. ODP Sci. Results* 178, 1–40.
- Barker, P.F., Camerlenghi, A., Acton, G.A., 1999. Antarctic glacial history and sea-level change. *Proc. ODP Init. Results* 178.
- Bart, P.J., Anderson, J.B., 2002. Relative temporal stability of the Antarctic ice sheets during the late Neogene based on the minimum frequency of outer shelf grounding events. *Earth Planet. Sci. Lett.* 182, 259–273.
- Borradaile, G.J., 1988. Magnetic susceptibility, petrofabrics and strain. *Tectonophysics* 156, 1–20.



- Camerlenghi, A., Crise, A., Pudsey, A.C., Accerboni, E., Laterza, R., Rebesco, M., 1997a. Ten-month observation of the bottom current regime across a sediment drift of the Pacific margin of the Antarctic Peninsula. *Antarct. Sci.* 9, 426–433.
- Camerlenghi, A., Rebesco, M., Pudsey, C.J., 1997b. High Resolution Terrigenous Sedimentary Record of a Sediment Drift on the Antarctic Peninsula Pacific Margin. *The Antarctic Region: Geological Evolution and Processes*, 705–710.
- Constable, C., Tauxe, L., 1990. The bootstrap for magnetic susceptibility tensors. *Jour. Geophys. Res.* 95, 8383–8395.
- Copons, R., Parés, J.M., Dinarès-Turell, J., Bordonau, J., 1997. Sampling induced AMS in soft sediments: a case study in Holocene glaciolacustrine rhythmites from Lake Barrancs (Central Pyrenees, Spain). *Phys Chem. Earth* 22, 137–141.
- Ellwood, B.B., Ledbetter, M.T., 1977. Antarctic Bottom Water fluctuations in the Vema Channel: effects of velocity changes on particle alignment and size. *Earth Planet. Sci. Lett.* 35, 189–198.
- Ellwood, B.B., Ledbetter, M.T., 1979. Paleocurrent Indicators in Deep-Sea Sediment. *Science* 203, 1335–1337.
- Ellwood, B.B., Ledbetter, M.T., Johnson, D.A., 1979. Sedimentary fabric: a tool to delineate a high-velocity zone within a deep western Indian Ocean bottom current. *Mar. Geol.* 33, M51–M55.
- Graham, J.W., 1954. Magnetic susceptibility anisotropy, an unexploited petrofabric element. *Geol. Soc. Amer. Bull.* 65, 1257–1258.
- Guyodo, Y., Acton, G.D., Brachfeld, S., Channell, J.E.T., 2001. A sedimentary paleomagnetic record of the Matuyama chron from the Western Antarctic margin (ODP Site 1101). *Earth Planet. Sci. Lett.* 191, 61–74.
- Hassold, N.J.C., 2006. Late Miocene to Recent changes in Abyssal Current strength: Views From the North Atlantic and the Pacific Margin of Antarctica. Ph.D., University of Michigan, Ann Arbor, Michigan.
- Hassold, N.J.C., Rea, D.K., van der Pluijm, B.A., Parés, J.M., Gleason, J.D., Ravelo, A.C., 2006. Late Miocene to Pleistocene paleoceanographic records from the Feni and Gardar Drifts: Pliocene reduction in abyssal flow. *Palaeogeogr. Palaeoclim. Palaeoecol.* 236, 290–301. doi: 210.1016/j.palaeo.2005.1011.1011.
- Hernández-Molina, F.J., Larter, R.D., Rebesco, M., Maldonado, A., 2006. Miocene reversal of bottom water flow along the Pacific Margin of the Antarctic Peninsula: stratigraphic evidence from a contourite sedimentary tail. *Mar. Geol.* 228, 93–116.
- Hounslow, M.W., 1985. Magnetic fabric arising from paramagnetic phyllosilicate minerals in mudrocks. *J. Geol. Soc. London* 142, 995–1006.
- Housen, B.A., van der Pluijm, B.A., 1990. Chlorite control of correlations between strain and anisotropy of magnetic susceptibility. *Phys. Earth Planet. Inter.* 61, 315–323.
- Hrouda, F., 1982. Magnetic anisotropy of rocks and its application in geology and geophysics. *Geophys. Surv.* 5, 37–82.
- Ising, G., 1942. On the magnetic properties of varved clay. *Ark. Mat. Astron. Fys.* 29a, 1–37.
- Jelinek, V., 1978. Statistical processing of anisotropy of magnetic susceptibility measured on groups of specimens. *Studia Geophys. et Geol.* 22, 50–62.
- Jelinek, V., 1981. Characterization of the magnetic fabrics of rocks. *Tectonophysics* 79, T63–T67.
- Joseph, L.H., Rea, D.K., van der Pluijm, B.A., 1998. Use of grain size and magnetic fabric analyses to distinguish among depositional environments. *Paleoceanography* 13, 491–501.
- Joseph, L.H., Rea, D.K., van der Pluijm, B.A., 2004. Neogene history of the Deep Western Boundary Current at Rekohu sediment drift, Southwest Pacific (ODP Site 1124). *Mar. Geol.* 205, 185–206.
- Kent, D.V., Lowrie, W., 1975. Magnetic susceptibility anisotropy of deep-sea sediment. *Earth Planet. Sci. Lett.* 28, 1–12.
- Kirschvink, J.L., 1980. The least-squares line and plane and the analysis of paleomagnetic data. *Geophys. J.R. Astron. Soc.* 62, 699–718.
- Kodama, K.P., Sun, W.W., 1990. SEM and magnetic fabric study of a compacting sediment. *Geophys. Res. Lett.* 17, 795–798.
- Ledbetter, M.T., Ellwood, B.B., 1980. Spatial and temporal changes in bottom-water velocity and direction from analysis of particle size and alignment in deep-sea sediment. *Mar. Geol.* 38, 245–261.
- Liu, B., Saito, Y., Toshitsugu, Y., Abdeldayem, A., Oda, H., Hori, K., Zhao, Q., 2001. Paleocurrent analysis for the Late Pleistocene–Holocene incised-valley fill of the Yangtze delta, China by using anisotropy of magnetic susceptibility data. *Mar. Geol.* 176, 175–189.
- McDonald, W.D., Ellwood, B.B., 1987. Anisotropy of magnetic susceptibility: Sedimentological, igneous and structural-tectonic applications. *Rev. Geophys.* 25, 905–909.
- Neves, S.P., Araújo, A.M.B., Correia, P.B., Mariano, G., 2003. Magnetic fabrics in the Cabanas Granite (NE Brazil): interplay between emplacement and regional fabrics in a dextral transpressive regime. *J. Struct. Geol.* 25, 441–453.
- Nye, J.F., 1957. *The Physical Properties of Crystals*. Clarendon Press, Oxford. 322 pp.
- Parés, J.M., van der Pluijm, B.A., 2003. Magnetic fabrics and strain in pencil structures of the Knobs Formation, Valley and Ridge Province, US Appalachians. *J. Struct. Geol.* 25, 1349–1358.
- Parés, J.M., van der Pluijm, B.A., Dinarès-Turell, J., 1999. Evolution of magnetic fabrics during incipient deformation of mudrocks (Pyrenees, northern Spain). *Tectonophysics* 307, 1–14.
- Park, C.K., Doh, S.J., Suk, D.W., Kim, K.H., 2000. Sedimentary fabric on deepsea sediments from KODOS area in the eastern Pacific. *Mar. Geol.* 171, 115–126.
- Pudsey, C.J., 2001. Neogene record of Antarctic Peninsula glaciation in continental rise sediments: ODP Leg 178, Site 1095. *Proc. ODP Sci. Results* 178, 1–25.
- Rebesco, M., Camerlenghi, A., Volpi, V., Neagu, C., Accettella, D., Lindberg, B., Corva, A., Zgur, F., 2007. Interaction of processes of importance of contourites: insights from the detailed morphology of sediment Drift 7, Antarctica. In: Viana, A., Rebesco, M. (Eds.), *Economic and Palaeoceanographic Importance of Contourite Deposits*. *GSL Special Publ.*, vol. 276, pp. 95–110.
- Rees, A.I., Woodall, W.A., 1975. The magnetic fabric of some laboratory-deposited sediments. *Earth Planet. Sci. Lett.* 25, 121–130.
- Richter, C., van der Pluijm, B.A., Housen, B., 1993. The quantification of crystallographic preferred orientation using magnetic anisotropy. *J. Struct. Geol.* 15, 113–116.
- Scott, R.G., Benn, K., 2001. Peak-ring rim collapse accommodated by impact melt-filled transfer faults, Sudbury impact structure, Canada. *Geology* 29, 747–750.
- Tarling, D.H., Hrouda, F., 1993. *The Magnetic Anisotropy of Rocks*. Chapman and Hall, New York, p. 217.
- Tauxe, L., 1998. *Paleomagnetic Principles and Practice*. Kluwer Academic Publishers, p. 299.
- Uenzelmann-Neben, G., 2006. Depositional patterns at Drift 7, Antarctic Peninsula: Along-slope versus down-slope sediment transport as indicators for oceanic currents and climatic conditions. *Mar. Geol.* 233, 49–62.
- Zijderveld, J.D.A., 1967. A.C. demagnetization of rocks: analysis of results. In: Collinson, D.W., Runcorn, S.K., Creer, K.M. (Eds.), *Methods in Paleomagnetism*. Elsevier, New York, pp. 254–286.